

X-RAYS FROM SUPERNOVA SHOCKS IN DENSE MASS LOSS

Roger A. Chevalier and Christopher M. Irwin

*Department of Astronomy, University of Virginia, P.O. Box 400325,
Charlottesville, VA 22904-4325; rac5x@virginia.edu*

ABSTRACT

Type II_n and related supernovae show evidence for an interaction with a dense circumstellar medium that produces most of the supernova luminosity. X-ray emission from shock heated gas is crucial for the energetics of the interaction and can provide diagnostics on the shock interaction. Provided that the shock is at an optical depth $\tau_w \lesssim c/v_s$ in the wind, where c is the speed of light and v_s is the shock velocity, a viscous shock is expected that heats the gas to a high temperature. For $\tau_w \gtrsim 1$, the shock wave is in the cooling regime; inverse Compton cooling dominates bremsstrahlung at higher densities and shock velocities. Although $\tau_w \gtrsim 1$, the optical depth through the emission zone is $\lesssim 1$ so that inverse Compton effects do not give rise to significant X-ray emission. The electrons may not reach energy equipartition with the protons at higher shock velocities. As X-rays move out through the cool wind, the higher energy photons are lost to Compton degradation. If bremsstrahlung dominates the cooling and Compton losses are small, the energetic radiation can completely photoionize the preshock gas. However, inverse Compton cooling in the hot region and Compton degradation in the wind reduce the ionizing flux, so that complete photoionization is not obtained and photoabsorption by the wind further reduces the escaping X-ray flux. We conjecture that the combination of these effects led to the low observed X-ray flux from the optically luminous SN 2006gy.

Subject headings: circumstellar matter — shock waves — supernovae: general — supernovae: individual (SN 2006gy) — X-rays: general

1. INTRODUCTION

There is increasing evidence for supernova shock waves propagating in dense, optically thick, mass loss regions. Type II_n supernovae, which have narrow lines of hydrogen and

other species in their spectra (Schlegel 1990), typically have light curves where circumstellar interaction provides the power (e.g., Chugai 1992). The lines are indicative of continuing circumstellar interaction and the luminosity implies a high circumstellar density. Narrow H lines with broad, symmetric wings observed at early times can be interpreted as the result of electron scattering in a medium with optical depth of 3 – 4 (Chugai 2001). Type II_n spectral features have been observed in number of highly luminous supernovae, including SN 2006gy (Smith et al. 2007; Ofek et al. 2007). SN 2006gy, which was especially luminous in the optical, had an X-ray luminosity (or upper limit) that was orders of magnitude below its optical luminosity (Smith et al. 2007; Ofek et al. 2007); the question arises of whether the lack of a high X-ray luminosity is consistent with strong circumstellar interaction (Katz et al. 2011).

There is the potential for X-ray emission provided that there is a viscous shock wave that heats the gas in the circumstellar interaction. A viscous shock front is expected to form in a dense wind provided the optical depth in the external medium $\tau \lesssim c/v_s$, where v_s is the shock velocity (Ofek et al. 2010; Chevalier & Irwin 2011; Nakar & Sari 2010). At larger optical depths the shock wave is mediated by radiation provided that the ratio of radiation to matter pressure is > 4.45 in the downstream region (Weaver 1976), which is the case for the shocks considered here. There is thus the potential for hot gas and its emission from shock waves in moderately optically thick regions (Katz et al. 2011). Here we consider the X-ray emission from shocks in dense circumstellar regions, concentrating on the optically thick case. Any emitted X-ray emission has the possibility of being scattered or absorbed, changing both the supernova surroundings and the escaping X-ray radiation. An understanding of how the shock power is eventually radiated is crucial for understanding multiwavelength observations of these events.

We discuss the shock structure and X-ray emission in Section 2 and the implications for observations in Section 3.

2. SHOCK PROPERTIES AND X-RAY EMISSION

We assume that the mass loss can be described by a steady wind flow; the actual mass loss is unlikely to be steady, but this case should illustrate the basic physical situation. If the mass loss at rate \dot{M} is in a steady wind at a velocity v_w , the density $\rho_w = \dot{M}/4\pi r^2 v_w \equiv D r^{-2}$ can be specified by a density parameter, D_* , scaled to a $\dot{M} = 10^{-2} M_\odot \text{ yr}^{-1}$ and $v_w = 10 \text{ km s}^{-1}$ wind so that $\rho_w = 5.0 \times 10^{16} D_* r^{-2}$ in cgs units. The optical depth in the wind to the dense shell position R is $\tau_w = 1.7 \times 10^{16} k D_* / R$ where k is the opacity κ in units of $0.34 \text{ cm}^2 \text{ g}^{-1}$, appropriate for electron scattering with $n_{He}/n_H = 0.1$. If the expansion of R

can be expressed $R \sim t^m$ where t is the age (Chevalier & Fransson 2003; Chevalier & Irwin 2011), we have $v_s = mR/t$ so that

$$D_* = 0.06v_{s4}\tau_w k^{-1}(t/10 \text{ day}), \quad (1)$$

where v_{s4} is the expansion velocity of the shell v_s in units of 10^4 km s^{-1} and $m = 0.8$ has been assumed. This relation with $\tau_w = 1$ is shown in Fig. 1, which also shows the line $\tau_w = c/v_s$ above which a viscous shock does not form. In the figure, and in the following, we assume $k = 1$.

2.1. Radiation from the Shocked Region

To give an estimate of the shock velocity, we note that for the supernova model used by Chevalier & Irwin (2011) ($\rho \propto r^{-7}$ outer density profile), the velocity of gas at the reverse shock wave is $6.3 \times 10^3 E_{51}^{0.2} M_{e1}^{-0.2} D_*^{-0.2} (t/10 \text{ day})^{-0.2} \text{ km s}^{-1}$, where E_{51} is the energy in units of 10^{51} ergs and M_{e1} is the ejecta mass in units of $10 M_\odot$. The velocity v of the interaction shell is also the shock velocity v_s if the velocity of matter immediately ahead of the shock is negligible. There are two reasons that v_s might be less than v . One is that the presupernova wind has a significant velocity. Wind velocities deduced from narrow H α line features in Type II n supernovae are generally in the range $100 - 1000 \text{ km s}^{-1}$ (Table 5 of Kiewe et al. 2012). Second, there may be radiative acceleration of the mass loss gas.

To estimate the acceleration, we assume that the forward shock velocity is $\sim v$ and that the shock wave cools rapidly (compared to the age). These assumptions should give the maximum luminosity and thus the maximal effect of radiative acceleration. The luminosity in this case is $L_c = 2\pi R^2 \rho_{w0} v^3$, where ρ_{w0} is the wind density immediately ahead of the shock wave. The acceleration is $a_{rad} = L\kappa/4\pi R^2 c$, where c is the speed of light, so that the gas is accelerated to a velocity

$$v_{rad} = a_{rad} t \approx \frac{\rho_{w0} v^2 m R \kappa}{2c}. \quad (2)$$

If we normalize to the shock velocity,

$$\frac{v_{rad}}{v} = \frac{m D v \kappa}{2 R c} = \frac{m v}{2 c} \tau_w. \quad (3)$$

The result is that $v_{rad} \sim v$ if $\tau_w \sim c/v$. The formation of a viscous shock requires that $\tau_w \lesssim c/v_s$, so we expect significant acceleration near the time of shock breakout, if it occurs in the wind region, and declining acceleration at lower optical depths. The breakout radiation from a hot shell of radiation can also accelerate the wind gas, but the luminosity of this event

is comparable to the luminosity that might be generated by the continuing shock interaction (Chevalier & Irwin 2011). Katz et al. (2011) obtain a similar result for the acceleration by breakout radiation and note that the shock is collisionless. Since the acceleration is important only at fairly large optical depth and we will find that X-rays do not escape at those depths, we neglect the acceleration here.

The cooling processes for the postshock hot gas are expected to be bremsstrahlung and inverse Compton cooling. At the high densities of interest here, the dominant cooling emission is from the forward shock region. X-ray emission from supernovae is often discussed in terms of the softer reverse shock emission (Chevalier & Fransson 2003). However, as the density increases, the reverse shock emission becomes limited by rapid cooling at a lower circumstellar density than at the forward shock. When both the forward and reverse shocks are in the radiative regime, the ratio of forward to reverse shock power is $2(n - 3)^2 / (n - 4)$, where n is the supernova density power law index (Chevalier & Fransson 2003). For $n = 7$, the ratio is 11. In addition, the dense shell that forms between the shock fronts can absorb X-ray emission produced at the reverse shock. In the noncooling regime, the bremsstrahlung emission from the forward shock region is (Chevalier & Fransson 2003)

$$L_b = 3 \times 10^{45} D_*^2 (t/10 \text{ day})^{-1} \text{ erg s}^{-1}. \quad (4)$$

In the cooling regime, the luminosity is

$$L_c = 3.1 \times 10^{44} D_* v_{s4}^3 \text{ erg s}^{-1}, \quad (5)$$

where v_{s4} is the shock velocity in units of 10^4 km s^{-1} . The actual luminosity cannot be greater than that in the cooling case. The cooling condition is that $L_b > L_c$, or

$$D_* > 0.1 v_{s4}^3 (t/10 \text{ day}). \quad (6)$$

The cooling condition is shown in Fig. 1; it is close to where the medium is optically thick.

Since the two sources of luminosity for inverse Compton cooling (shock breakout emission and emission from continuing interaction) are comparable at early times and the continuing interaction eventually can dominate, here we consider only the interaction luminosity source. If the forward shock is cooling, the postshock luminosity is $L_c = 2\pi R^2 \rho_0 v_s^3$. We assume that a fraction f of this luminosity is reradiated as approximately blackbody thermal radiation and take $f = 0.5$ as a reference value; backscattering of the radiation can cause deviations from this value. In the optically thick regime ($\tau_w > 1$), the energy density in radiation is thus

$$u_{rad} \approx \frac{f L_c}{4\pi r^2 c} \tau_w. \quad (7)$$

The inverse Compton energy loss per unit volume is

$$\Lambda_C = 4u_{rad}cn_e\sigma_T\frac{k_B T_e}{m_e c^2}, \quad (8)$$

where n_e is the electron density in the hot gas, σ_T is the Thomson cross section, k_B is Boltzmann’s constant, m_e is the electron mass, and T_e is the electron temperature. In the radiative, optically thick regime, the ratio of the bremsstrahlung cooling rate to the Compton cooling rate is

$$\frac{\Lambda_{br}}{\Lambda_C} \approx 0.7 \left(\frac{f}{0.5} \right)^{-1} v_{s4}^{-4} \tau_w^{-1}, \quad (9)$$

where equation (3-56) of Spitzer (1978) was used for Λ_{br} . The boundary between the cooling mechanisms is shown in Fig. 1.

Moving to the non-cooling case, we note that $L_c \propto D$ in the cooling case, but the luminosity of the shell $L = V\Lambda_{br} \propto D^2$ in the noncooling case, where V is the emitting volume of the hot gas. We again assume that the supernova luminosity is primarily from circumstellar interaction so that the photospheric luminosity is $fV\Lambda_{br}$. More specifically, we find

$$\frac{\Lambda_{br}}{\Lambda_C} \approx \frac{1}{4f\tau_0} \left(\frac{kT}{m_e c^2} \right)^{-1} = 2.1 \left(\frac{f}{0.5} \right)^{-1} v_{s4}^{-2} \tau_0^{-1}. \quad (10)$$

The electron scattering optical depth through the hot shell, τ_0 , is the same as that through the preshock wind gas, τ_w , provided H and He are ionized and dominate the abundances, and the shell gas is noncooling. The value of τ_0 drops below unity in the noncooling regime. Inverse Compton cooling is important at higher shock velocities and wind densities (Fig. 1). This contrasts with the case where the radiation field is due to the supernova, independent of the circumstellar interaction, when bremsstrahlung emission becomes a more important coolant at high density (Fransson 1982). At the higher densities in our case, inverse Compton again becomes important due to the strong radiation field created by the interaction. As indicated in Fig. 1, the condition that the shock front be cooling merges with the transition between inverse Compton and bremsstrahlung cooling at higher shock velocities. The reason for the absence of a region in which the shock is non-cooling with cooling dominated by inverse Compton is our assumption that the supernova luminosity is produced by the shock interaction.

If the nuclei and electrons do not rapidly achieve equilibrium in the shock transition, the nuclei are heated to $T_p = 2.9 \times 10^9 v_{s4}^2$ K in the shock front. The balance of electron cooling by inverse Compton losses with heating by Coulomb collisions leads to a temperature $T_e \approx 7.1 \times 10^8 \epsilon_\gamma^{-2/5}$ K, where ϵ_γ is the fraction of the postshock energy density in radiation and a Coulomb logarithm of 30 is assumed (Katz et al. 2011); T_e may be higher if there is

collisionless heating of electrons. From equation (7), we have $\epsilon_\gamma \approx (\tau_w v_s/c)$, so that when the viscous shock first forms $\epsilon_\gamma \sim 1$, but it declines thereafter. The electrons are heated to their equilibrium value ($1.4 \times 10^9 v_{s4}^2$ K) when $\tau_w \approx 5.7 v_{s4}^{-1}$. Nonequilibrium is important only for high shock velocities (Fig. 1). The criterion for equilibrium when the cooling is dominated by bremsstrahlung at lower densities is the same as that discussed by Fransson (1982, equation 12) and is shown in Fig. 1.

For $\tau_w \lesssim 1$, bremsstrahlung is expected at close to the postshock temperature and, since the emission goes in toward the dense photosphere as well as outward, with a luminosity approximately equal to that from the photosphere. As the optical depth to the emission region increases, there is more of a chance of an outward going photon being scattered in toward the photosphere, so the hard X-ray luminosity declines relative to the photospheric emission. In the cooling case, the electron scattering optical depth through the hot, shocked region is $\tau_0 = n_e \sigma_T d$, where $d = (v_s/4)t_{cool}$ and $t_{cool} = (3/2)nk_B T/\Lambda$. If inverse Compton dominates the cooling and $\tau_w > 1$, Λ is given by equations (7) and (8), and we have

$$\tau_0 = \frac{3}{4f\mu\tau_w} \frac{m_e}{m_p} \left(\frac{c}{v_s}\right)^2 \approx \frac{0.6}{f\tau_w v_{s4}^2}, \quad (11)$$

where μ is the mean particle weight divided by the proton mass m_p . We thus find that $\tau_0 \lesssim 1$, so that a typical outgoing photon from the dense shell scatters at most once in the hot gas; since the electron energies are $\lesssim m_e c^2$, the photon energy is changed by a factor < 2 . For $\tau_w > 1$, photons can be scattered back through the hot region, but production of photons up to X-ray energies is not expected in this way because the ingoing photons are absorbed by the dense shell and ejecta. We thus expect that, in the regime where inverse Compton cooling dominates, the X-ray emission declines relative to emission at lower photon energies. This is also true when bremsstrahlung cooling dominates and $\tau_w > 1$ because initially outgoing photons can be scattered back across the emission region and absorbed in the dense shell.

2.2. Photon Interaction with the Preshock Wind

The X-ray radiation from the hot shell must escape through the cooler unshocked envelope of circumstellar gas. Both scattering and absorption of the photons can be important. Comptonization affects the escape of photons at the high energy end. The maximum energy is $\epsilon_{max} \approx m_e c^2 / \tau_{es}^2 = 511 / \tau_{es}^2$ keV, where the electron scattering optical depth $\tau_{es} = \tau_w$ for our assumptions. This result is due to the fact that electron recoil gives a change of photon wavelength $\sim h/m_e c$ for each scattering, where h is Planck's constant, and the number of scatterings is $\sim \tau_{es}^2$. Detailed calculations show that there is not a sharp cut-off at the energy, but the spectrum becomes steep (e.g., Fig. 15 of Kylafis & Lamb 1982). In Section 1, we

noted that a viscous shock could form at $\tau_w \approx c/v_s = 30v_{s4}^{-1}$ so that ϵ_{max} can be as small as $0.57v_{s4}^2$ keV. The emission from the hot gas goes into heating and ionization of the preshock gas until the shock wave reaches moderate optical depth.

Photoionization of the preshock medium is important for the absorption of X-rays from the shocked region. If the preshock medium is completely ionized, we expect relatively little absorption, while incomplete ionization leads to substantial absorption for our parameters. In considering the photoionization of the preshock gas, we will be assuming that the photoionization is determined by the current X-ray luminosity, i.e. that steady state conditions apply. This requires that the recombination time be less than the age, which is generally true for the high densities considered here.

If the medium is optically thin, photoionization is related to the ionization parameter $\xi = L/nr^2$ in cgs units, where n is the density and r is the distance from the luminosity source. For an r^{-2} density distribution, the ξ parameter is independent of radius. If we are in the cooling regime and the ionizing luminosity is βL_c , the ionization parameter is $\xi \approx 1 \times 10^4 \beta v_{s4}^3$, independent of D . For lower values of D in the non-cooling regime, we have $\xi \propto Dt^{-1}$. The ionization parameter is highest in the high density regime of interest here and drops at lower densities in the noncooling regime. Photoionization calculations have been previously carried out and we briefly summarize results for an emitting gas temperature of 10 keV, or $\sim 10^8$ K. For a value $\xi \sim 10^4$, the medium is completely ionized (Tarter et al. 1969; Hatchett et al. 1976; Kallman & McCray 1982). The elements C, N, and O are completely ionized for $\xi \gtrsim 100$; ionization of the heavier elements (S and Fe) requires $\xi > 10^3$ (Hatchett et al. 1976).

To extend these results to a hotter radiation field, we used the photoionization code CLOUDY (Ferland et al. 1998). We started by using a radiation field set by a $T = 10^8$ K bremsstrahlung spectrum; the results were consistent with those described above. We went to higher bremsstrahlung temperatures to allow for higher shock velocities; at $v_{s4} = 1$, the postshock temperature is $\sim 10^9$ K. At $\xi = 1000$, changing the bremsstrahlung temperature does not have much effect on ionization structure or T_e . For $\xi \lesssim 1000$, a higher temperature luminosity leads to a lower T_e and less ionization. But for $\xi \geq 1000$, a higher temperature luminosity produces a higher T_e and more ionization. For example, at $T = 10^8$ K, the CNO elements are completely ionized at $\xi = 100$, S becomes ionized at $\xi \sim 1000$, and everything is ionized at $\xi \sim 10^4$. However, for $T = 10^9$ K, CNO do not become ionized until $\xi \sim 500$, S still becomes ionized at $\xi = 1000$, but everything is ionized at $\xi \sim 5000$. These results can be understood since the ionization potential is $\propto Z^2$, where Z is the atomic number. The higher temperature emission has higher energy photons, which are less efficient at ionizing atoms with lower ionization potentials (compared to the photon energy), but are more effective at

ionizing atoms with high ionization potentials.

For $\tau_w \sim 1$, we expect that $\beta \sim 0.5$, and the value of ξ mainly depends on v_s . For $v_{s4} \geq 1$, the gas is completely ionized, while for $v_{s4} = 0.5$ only partial ionization is likely. Another issue is whether the preshock medium is optically thick in the photoionization continua, and the incident radiation field is depleted in crossing the circumstellar gas. Using the results of Tarter & Salpeter (1969), we find that at the higher temperatures of interest ($\sim 10^9$ K) for the ionizing radiation, photon depletion is negligible and ionization remains nearly constant with radius. At lower temperatures for the radiation ($\sim 10^8$ K), there is a transition to the Stromgren regime.

The situation changes if the wind is moderately optically thick to electron scattering. An effect of electron scattering is to reverse the motion of photons, so that the energy density of ionizing photons is increased; the time spent by photons in a region is increased by $\sim \tau_w$ (equation [7]), so that the rate of ionizations (and ξ) is increased by the same factor (e.g., Ross 1979). While this effect favors higher photoionization and the escape of X-rays, there are several effects that disfavor high X-ray emission. First, Compton degradation in the wind leads to the loss of the high energy photons, as discussed above; emission above 2 keV is suppressed when $\tau_w \sim 16$. Second, at moderate optical depths inverse Compton cooling tends to dominate bremsstrahlung (Fig. 1), so that X-ray emission is a smaller fraction of the shock power; inverse Compton is more important at higher shock velocities. In addition, initially outgoing X-ray photons have some chance of being scattered back and absorbed by the dense shell. Finally, at optical depths $\gtrsim 10$, these two effects are likely to be larger than the increase in the ionizing radiation field, so that the ionization parameter is decreased and there is an increased chance of photoabsorption of the X-ray emission. Photoabsorption is important at low X-ray energies while Compton degradation is important at high X-ray energies. An accurate calculation of the X-ray emission is complicated and beyond the current paper. An analogous physical situation is X-ray emission from optically thick accretion onto white dwarfs (Kylafis & Lamb 1982). The photon trapping limit $\tau_w = c/v_s$ here corresponds to an accretion rate at the Eddington limit in the accretion case. A difference is that the emission from the white dwarf surface can maintain complete ionization of the preshock gas, which is not necessarily the case here.

3. IMPLICATIONS FOR OBSERVATIONS

Most of the X-ray observations of Type IIn supernovae in dense media are an age > 1 yr and sometimes much greater, so that the objects do not fall in the parameter space shown in Fig. 1. However, SN 2006gy, with an estimated $D_* \approx 10$ (Smith & McCray 2007;

Chevalier & Irwin 2011), was observed with *Chandra* on 2006 Nov 14, at an age of 3 – 4 months (Smith et al. 2007; Ofek et al. 2007). Smith et al. (2007) inferred a detection, with all counts at energies < 2 keV and an unabsorbed 0.5–2 keV luminosity of 1.65×10^{39} erg s $^{-1}$ assuming $T = 1$ keV. From the same data, Ofek et al. (2007) inferred a nondetection with an upper limit of 1.6×10^{40} erg s $^{-1}$, assuming a photon index of 1.8. In either case, the X-ray luminosity was much less than the observed photospheric luminosity of $\sim 3 \times 10^{44}$ erg s $^{-1}$ (Smith et al. 2010). In the model of Chevalier & Irwin (2011) for SN 2006gy, the shock wave radiation broke out in the mass loss region, so the optical depth outside the shock was initially c/v_s . The parameters for the X-ray observation give $D_*(t/10 \text{ day})^{-1} \sim 1$, near the $\tau_w = c/v_s$ line in Fig. 1. Smith et al. (2010) estimate $v_s \approx 4000 - 5000$ km s $^{-1}$ near the time of peak optical luminosity so, as discussed in Section 2.2, Comptonization by itself could limit the escaping photons to < 0.14 keV, and the loss of ionizing radiation would allow photoabsorption.

Our discussion suggests the following sequence, as the density of surrounding mass loss increases. At low density, the optical luminosity is dominated by radioactivity and shock heating of the progenitor; X-ray emission from interaction is initially a small part of the luminosity, although it might become a larger part at late times when other power sources fade. As the optical depth in the wind approaches unity, interaction typically dominates the power input and X-ray emission can be a significant part of the power. At higher densities, the X-ray emission falls relative to the optical luminosity because of inverse Compton cooling of the shocked region, Compton degradation in the wind, and photoabsorption.

We thank Claes Fransson for discussions and the referee for useful comments. This research was supported in part by NSF grant AST-0807727.

REFERENCES

- Chevalier, R. A., & Irwin, C. M. 2011, *ApJ*, 729, L6
- Chevalier, R. A., & Fransson, C. 2003, in *Supernovae and Gamma-Ray Bursters*, ed. K. W. Weiler (Berlin: Springer), 171
- Chugai, N. N. 1992, *Soviet Ast.*, 36, 63
- Chugai, N. N. 2001, *MNRAS*, 326, 1448
- Ferland, G. J., Korista, K. T., Verner, D. A., et al. 1998, *PASP*, 110, 761

- Fransson, C. 1982, *A&A*, 111, 140
- Hatchett, S., Buff, J., & McCray, R. 1976, *ApJ*, 206, 847
- Katz, B., Sapir, N., & Waxman, E. 2011, preprint, arXiv:1106.1898
- Kallman, T. R., & McCray, R. 1982, *ApJS*, 50, 263
- Kiewe, M., Gal-Yam, A., Arcavi, I., et al. 2012, *ApJ*, 744, 10
- Kylafis, N. D., & Lamb, D. Q. 1982, *ApJS*, 48, 239
- Nakar, E., & Sari, R. 2010, *ApJ*, 725, 904
- Ofek, E. O., Cameron, P. B., Kasliwal, M. M., et al. 2007, *ApJ*, 659, L13
- Ofek, E. O., Rabinak, I., Neill, J. D., et al. 2010, *ApJ*, 724, 1396
- Ross, R. R. 1979, *ApJ*, 233, 334
- Schlegel, E. M. 1990, *MNRAS*, 244, 269
- Smith, N., & McCray, R. 2007, *ApJ*, 671, L17
- Smith, N., Li, W., Foley, R. J., et al. 2007, *ApJ*, 666, 1116
- Smith, N., Chornock, R., Silverman, J. M., Filippenko, A. V., & Foley, R. J. 2010, *ApJ*, 709, 856
- Spitzer, L. 1978, *Physical processes in the interstellar medium* (New York: Wiley-Interscience)
- Tarter, C. B., & Salpeter, E. E. 1969, *ApJ*, 156, 953
- Tarter, C. B., Tucker, W. H., & Salpeter, E. E. 1969, *ApJ*, 156, 943
- Weaver, T. A. 1976, *ApJS*, 32, 233

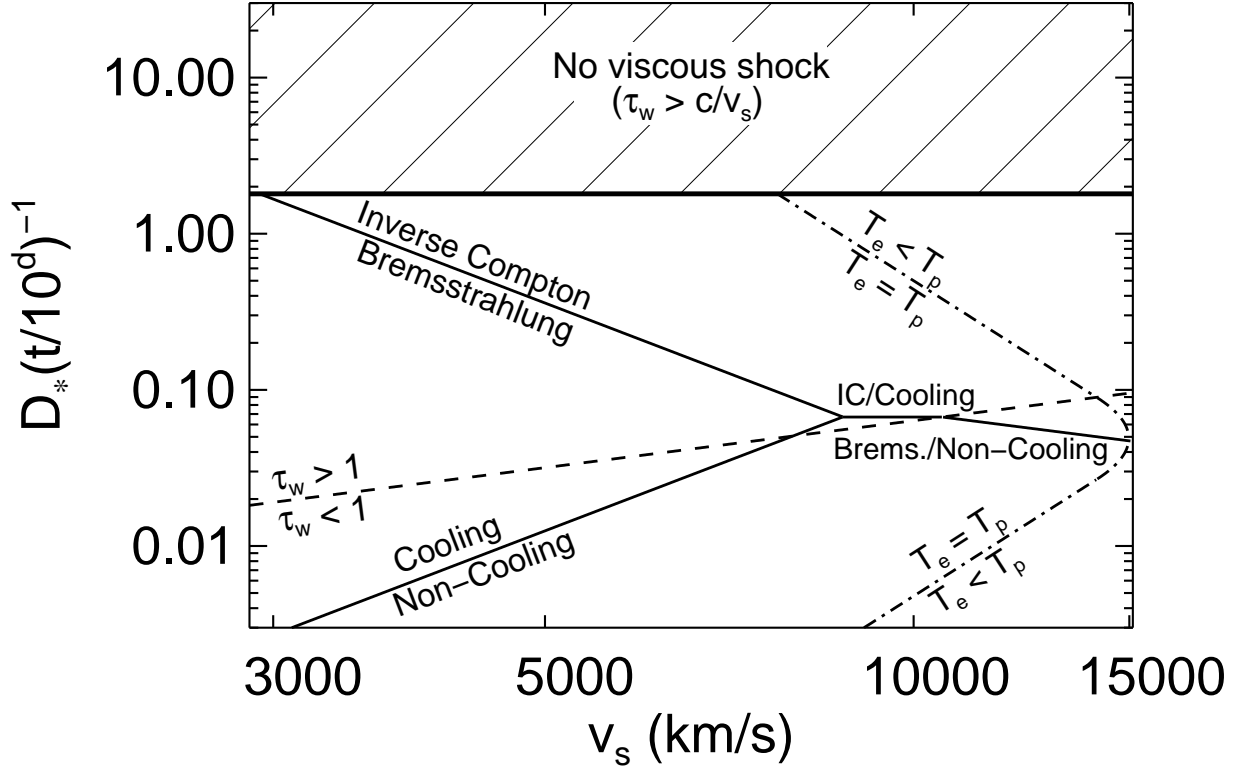


Fig. 1.— Regimes of shock structure in terms of wind density/age vs. shock velocity. The lines in the figure mark the limits of *a*) presence of viscous shock (thick solid line), *b*) optical depth unity (dashed), *c*) rapid cooling (solid), *d*) cooling by inverse Compton vs. bremsstrahlung (solid), and *e*) electron-proton equilibration (dash-dot).